Proyecto Fin de Carrera

2D Eulerian-Eulerian Shocked Particle-Laden Flows: Normal Shockwave interaction with a Cloud of Particles.

Author:
Alfonso de las Heras Muñoz

Advisor:
Dr. Gustaaf Jacobs
Dr. Sean Davis

A thesis submitted in fulfilment of the requirements
for the Master's of Industrial Engineering
in

Department of Aerospace Engineering
San Diego State University
Departamento de Ingeniería Energética y Fluidodinámica
Universidad de Valladolid

Universidad de Valladolid

July 2015

,

I would like to dedicate this thesis to my loving family
because they made it possible...

Abstract:

The 2D Eulerian-Eulerian model is implemented in a high-speed particle-laden flow for the first time to elucidate the interaction between a right-running shock and a cloud of particles. The Eulerian particle phase is modeled as a compressible fluid, which reduces the computational cost of modeling large amount of particles. Source terms in the Eulerian governing equations allow for the tranfer of momentum and energy between the phases.

Second moments provide information about the inertial effects and create a non-linear system of equations. High-order, finite difference, WENO schemes are able to capture the shock with the neccesary numerical dissipation to assure the convergence and stability of the method but obtaining the enough accuracy in the smooth areas of the solution.

Acknowledgements

First, I would like to thank Mª Teresa for giving me the oportunity to come to San Diego for this year as well as to Gustaaf Jacobs for guiding me throughout this project. I would also like to thank Sean Davis for all the time he spent helping me with mmy work.

I would want to remember all the people I shared with this experience, specially those who came with me from Valladolid, Eduardo and Ignacio, as well as Wouter, because they have been like my family along this year; my roomates Francesco and Vincenzo for all the time we shared together and my labmates because they were always willing to help me out.

Last but not least, I want to heartily thank my family; my parents, Constantino and Blanca, and my sister, Cristina; for all the support and understanding they gave me.

Contents

List of Figures

List of Tables

Symbols

x, y	Position
x_p	Particle position
ρ	Fluid density
u	Fluid velocity in x
v	Fluid velocity in y
$Temp$	Fluid temperature
p	Fluid pressure
H	Enthalpy
c	Sound speed
M	Mach number
γ	Ratio gas capacities
β	Ratio of particle heat capacity to fluid heat capacity at constant pressure
τ_p	Particle relaxation time constant
τ_T	Particle thermal relaxation time constant
ρ_f	Reference density
U_f	Reference velocity in x
V_f	Reference velocity in y
M_f	Reference Mach number
L_{fx}	Reference length in x
L_{fy}	Reference length in y
T_f	Reference Temperature
M_p	Mass of a single particle
ϕ	Particle number density
u_p	Particle velocity in x
v_p	Particle velocity in y

θ	Particle temperature
W	Fine-grained phase-space density function
δ	Dirac delta function
H_Δ	Kernel function
$*$	Dimensional variables
λ_i	Eigenvalues of Jacobian matrix

Chapter 1

Introduction

Particle-Laden Flows are composed by two phases. The Euler Phase or also named Carrier Phase which is usually a gas and the Particle Phase or Disperse Phase, which is composed by small, immiscible particles in suspension inside the Carrier Phase. These phases are together and mixed. Particle-Laden flows are present in such environments as volcanic eruptions, pollution dispersion in the atmosphere or fluidization in combustion processes. Some industrial applications can be the aerosol deposition in spray medication, turbulent mixing of liquid fuel particles with air in an automobile's engine or fuel spray in a gas turbine. [1], [5].

This problem has been traditionally faced with a classical Euler approach for the Carrier Phase, using the Navier-Stokes equations which focuses on an specific location or Control Volume through which the fluid passes by; and a Lagrangian approach for the Disperse Phase, where the observer follows an individual fluid parcel as it moves through space and time. This is called the E-L model. E-L model is explained in [3].

Since the Particles are usually considered spherical and light enough to behave as a fluid, an Eulerian treatment of the disperse Phase is sensible. Secondly, when the porblem requires to solve a large amount of particles, Lagrangian frame become a very computationally expensive method. In this thesis, and Eulerian Eulerian, E-E model is developed and, as we will see, the Euler this approach for the problem, which basically means modelling the particles as a second fluid inside the Carrier Phase, is a good method as well.

An analysis of the results are presented, using a WENO method to solve it. This method is very suitable for the problem beacuse of the high accuracy in smooth areas providing the neccessary dissipation for capturing shockwaves. Further information about WENO schemes will be provided by [3],[4].

First, we introduce the physical model: The Carrier Phase, the Disperse Phase and the coupling between them. In Chapter 3, the numerical methods used to solve the problem will be discussed. In section Chapter 4, the problem is solved, setting a Normal Shockwave interacting with a rectangular cloud of particles. Plots representing the main variables of the problem are shown and results are discussed. Finally, in section Chapter 5, conclusions and future directions are presented.

Chapter 2

Governing Equations

2.1 Carrier Phase

The following assumptions are made to derive the Euler equations:
• The fluid is Newtonian.
• The fluid is continuous, so the smallest length scale of motion of the fluid is very large compared with the molecular motion.
• It is a convection dominated flow, hence the inviscid Euler equations are used.
• The fluid is considered an idel gas. Intermolecular forces are negligible and the equation of state is given by the ideal gas law.

The first step is to non-dimensionalize the equations that are given. We normalize them using a reference length L_f, reference density ρ_f, reference velocity U_f and V_f and reference temperature T_f. The non-dimensional variables are the following:

$$x = \frac{x^*}{L_{fx}}, \qquad y = \frac{y^*}{L_{fy}}, \tag{2.1}$$

$$u = \frac{u^*}{U_f^*}, \qquad v = \frac{v^*}{V_f^*}, \tag{2.2}$$

$$\rho = \frac{\rho^*}{\rho_f^*}, \qquad T = \frac{T^*}{T_f^*}, \tag{2.3}$$

$$p = \frac{p^*}{\rho_f^* U_f^{*2}}, \qquad t = \frac{t^* U_f^*}{L_f^*} \tag{2.4}$$

. From the non-dimensional variables, we can build the Euler equations,

$$\frac{\partial Q_f}{\partial t} + \frac{\partial F_f}{\partial x} + \frac{\partial G_f}{\partial y} = 0 \tag{2.5}$$

$$Q_f = \begin{bmatrix} \rho \\ \rho u \\ \rho v \\ E \end{bmatrix} \quad , \quad F_f = \begin{bmatrix} \rho u \\ \rho u^2 + p \\ \rho uv \\ (E+p)u \end{bmatrix} \quad , \quad G_f = \begin{bmatrix} \rho v \\ \rho uv \\ \rho v^2 + p \\ (E+p)v \end{bmatrix} \tag{2.6}$$

Where Q contains the conservative variables, while F and G are the fluxes in x and y respectively. If we apply the Chain Rule, we obtain the characteristic form

$$\frac{\partial Q_f}{\partial t} + A_f \frac{\partial Q_f}{\partial x} + B_f \frac{\partial Q_f}{\partial y} = 0, \tag{2.7}$$

where A_f and B_f are the Jacobian Matrix of the system in x and y dimensions. In the x-direction, the jacobian matrix is

$$A_f = \begin{bmatrix} 0 & 1 & 0 & 0 \\ \frac{1}{2}[(\gamma-3)u^2 + (\gamma-1)v^2] & (3-\gamma)u & -(\gamma-1)v & \gamma-1 \\ -uv & v & u & 0 \\ \gamma uE + (\gamma-1)u(u^2+v^2) & \gamma E - \frac{\gamma-1}{2}(v^2+3u^2) & -(\gamma-1)uv & \gamma u \end{bmatrix}, \tag{2.8}$$

and the corresponding eigenvalues and eigenvectors associated,

$$\lambda_1 = u - c \quad , \quad \lambda_2 = u \quad , \quad \lambda_3 = u \quad , \quad \lambda_4 = u + c, \tag{2.9}$$

$$r_1 = \begin{bmatrix} 1 \\ u-c \\ v \\ H - uc \end{bmatrix}, \quad r_2 = \begin{bmatrix} 1 \\ u \\ v \\ \frac{1}{2}(u^2+v^2) \end{bmatrix}, \quad r_3 = \begin{bmatrix} 0 \\ 0 \\ 1 \\ v \end{bmatrix}, \quad r_4 = \begin{bmatrix} 1 \\ u+c \\ v \\ H + uc \end{bmatrix} \tag{2.10}$$

.

Similarly in the y-direction,

$$B_f = \begin{bmatrix} 0 & 0 & 1 & 0 \\ -uv & v & u & 0 \\ \frac{1}{2}[(\gamma-1)u^2 + (\gamma-3)v^2] & -(\gamma-1)u & (3-\gamma)v & \gamma-1 \\ -\gamma uE + (\gamma-1)v(u^2+v^2) & -(\gamma-1)uv & \gamma E - \frac{\gamma-1}{2}(u^2+3v^2) & \gamma v \end{bmatrix}, \tag{2.11}$$

and the corresponding eigenvalues and eigenvectors

$$\lambda_1 = v - c \quad , \quad \lambda_2 = v \quad , \quad \lambda_3 = v \quad , \quad \lambda_4 = v + c, \tag{2.12}$$

$$r_1 = \begin{bmatrix} 1 \\ u \\ v-c \\ H-vc \end{bmatrix}, \quad r_2 = \begin{bmatrix} 1 \\ u \\ v \\ \frac{1}{2}(u^2+v^2) \end{bmatrix}, \quad r_3 = \begin{bmatrix} 0 \\ 1 \\ 0 \\ u \end{bmatrix}, \quad r_4 = \begin{bmatrix} 1 \\ u \\ v+c \\ H+vc \end{bmatrix} \tag{2.13}$$

.

In order to close the system of equations, the Stagnation Energy equation is used

$$E = \frac{p}{\gamma - 1} + \frac{1}{2}(u^2 + v^2), \tag{2.14}$$

along the Ideal gas law.

$$p = \frac{\rho T}{\gamma} \tag{2.15}$$

2.2 Disperse Phase

The Particle-Phase equations in the Eulerian frame are derived from the Lagrangian equations of the position vector x_P, the velocity vector v_P and the temperature θ_P of a single particle. u is the fluid velocity vector and T corresponds to the fluid temperature. More detailed explanation is shown in [2].

$$\frac{dx_P}{dt} = v_P \tag{2.16}$$

$$\frac{dv_P}{dt} = \frac{1}{\tau_P}(u - v_P) \tag{2.17}$$

$$\frac{d\theta_P}{dt} = \frac{1}{\tau_T}(T - \theta_P) \tag{2.18}$$

In order to implement the Eulerian paticle phase equations, we need to derive a continuity variable. We use the Number Density Function ϕ.
A fine-grained phase-space density function is defined as,

$$W(x, v, \theta, t) = \delta[x - x_P(t)]\delta[v - v_P(t)]\delta[\theta - \theta_P(t)] \tag{2.19}$$

The fine grained phase-space densuty function verifies the Liouville equation in the phase space

$$\frac{\partial W}{\partial t} + \frac{\partial v_i W}{\partial x_i} - \frac{\partial}{\partial v_i}[\frac{(v_i - u_i)}{\tau_P} W] - \frac{\partial}{\partial \theta}[\frac{(\theta - T)}{\tau_P} W] = 0 \tag{2.20}$$

A spatial filtering operation is applied,

$$\bar{f}(x) = \int f(x') H_\Delta(x - x') dx', \tag{2.21}$$

where $\bar{f}(x)$ is the filtered value of $f(x)$, H_Δ the Kernel Function and Δ the size of the filter. This size is chosen small, in order to avoid subgrid-scale fluctuations. The filtered Liouvulle equation is

$$\frac{\partial \bar{W}}{\partial t} + \frac{\partial v_i \bar{W}}{\partial x_i} - \frac{\partial}{\partial v_i}[\frac{(v_i - u_i)}{\tau_P}\bar{W}] - \frac{\partial}{\partial \theta}[\frac{(\theta - T)}{\tau_P}\bar{W}] = 0, \tag{2.22}$$

where $\bar{W}$ is a coarse-grained fucntion with all the properties of a probability density function when the Kernel H_Δ is positive. The Number Density, ϕ, the Eulerian velocity and Eulerian temperature are obtained in terms of $\bar{W}$ as follows,

$$\bar{\phi} = \int \bar{W}(x, v, \theta, t) dv d\theta, \tag{2.23}$$

$$\bar{v_i} = \frac{1}{\bar{\phi}} \int v_i \bar{W}(x, v, \theta, t) dv d\theta, \tag{2.24}$$

$$\bar{\theta} = \frac{1}{\bar{\phi}} \int \theta \bar{W}(x, v, \theta, t) dv d\theta. \tag{2.25}$$

Using these equations and the definitions we obtain the governing equations for the Particle Phase:

$$\frac{\partial \bar{\phi}}{\partial t} + \frac{\partial \bar{\phi}\bar{v_i}}{\partial x_i} = 0, \tag{2.26}$$

$$\frac{\partial \bar{\phi}\bar{v_i}}{\partial t} + \frac{\partial \bar{\phi}\overline{v_i v_j}}{\partial x_j} = \frac{1}{\tau_P}\bar{\phi}(u_i - \bar{v_i}), \tag{2.27}$$

$$\frac{\partial \bar{\phi}\bar{\theta}}{\partial t} + \frac{\partial \bar{\phi}\theta\bar{v_i}}{\partial x_i} = \frac{1}{\tau_T}\bar{\phi}(T - \bar{\theta}), \tag{2.28}$$

$$\frac{\partial \bar{\phi}\overline{v_i v_j}}{\partial t} + \frac{\partial \bar{\phi}\overline{v_i v_j v_k}}{\partial x_k} = \frac{1}{\tau_P}\bar{\phi}(u_i\bar{v_j} + \bar{v_i}u_j - 2\overline{v_i v_j}), \tag{2.29}$$

$$\frac{\partial \bar{\phi}\overline{\theta v_i}}{\partial t} + \frac{\partial \bar{\phi}\overline{\theta v_i v_k}}{\partial x_k} = \frac{1}{\tau_P}\bar{\phi}(u_i\bar{\theta} - \overline{\theta v_j}) + \frac{1}{\tau_T}\bar{\phi}(T\bar{v_i} - \overline{\theta v_j}). \tag{2.30}$$

In order to close the system of equations, we model the third-order moments approximating:

$$\overline{v_i v_j v_k} - \overline{v_j v_k}\bar{v_i} - \overline{v_i v_j}\bar{v_k} - \overline{v_i v_k}\bar{v_j} + 2\bar{v_i}\bar{v_j}\bar{v_k} \approx 0, \tag{2.31}$$

$$\overline{\theta v_j v_k} - \overline{\theta v_k}\bar{v_i} - \overline{\theta v_j}\bar{v_k} - \overline{v_i v_k}\bar{\theta} + 2\bar{v_i}\bar{v_k}\bar{\theta} \approx 0. \tag{2.32}$$

For the 2D case, we introduce the sub-grid scale particle stress, σ_{ij}, and the sub-grid scale particle heat flux, qq_i. These terms capture information about the inertial effects,

$$\sigma_{ij} = \quad \overline{v_i v_j} - \bar{v_i}\bar{v_j}, \tag{2.33}$$

$$qq_i = \quad \overline{\theta v_i} - \bar{\theta}\bar{v_i}. \tag{2.34}$$

Once we have modelled the particle phase in the Eulerian frame, we can use the same governing equation as in the carrier phase, introducing the particle variables described before:

$$\frac{\partial Q_P}{\partial t} + \frac{\partial F_P}{\partial x} + \frac{\partial G_P}{\partial y} = 0 \tag{2.35}$$

where Q contains the conservative variables $\widetilde{\phi}$, $\widetilde{u_P}$, $\widetilde{v_P}$, $\widetilde{\theta}$, σ_{uu}, σ_{vv}, σ_{uv}, qq_u, qq_v while F and G are the fluxes in x and y direction respectively,

$$Q_P = \begin{bmatrix} \widetilde{\phi} \\ \widetilde{\phi}\widetilde{u_P} \\ \widetilde{\phi}\widetilde{v_P} \\ \widetilde{\phi}\widetilde{\theta} \\ \widetilde{\phi}(\sigma_{uu} + \widetilde{u_P}^2) \\ \widetilde{\phi}(\sigma_{uv} + \widetilde{u_P}\widetilde{v_P}) \\ \widetilde{\phi}(\sigma_{vv} + \widetilde{v_P}^2) \\ \widetilde{\phi}(qq_u + \widetilde{\theta}\widetilde{u_P}) \\ \widetilde{\phi}(qq_v + \widetilde{\theta}\widetilde{v_P}) \end{bmatrix} = \begin{bmatrix} Q_1 \\ Q_2 \\ Q_3 \\ Q_4 \\ Q_5 \\ Q_6 \\ Q_7 \\ Q_8 \\ Q_9 \end{bmatrix}, \tag{2.36}$$

$$F_P = \begin{bmatrix} Q_2 \\ Q_5 \\ Q_6 \\ Q_8 \\ -2{Q_2}^3/{Q_1}^2 + 3Q_2Q_5/Q_1 \\ 2Q_2Q_6/Q_1 + Q_3Q_5/Q_1 - 2Q_2^2Q_3/Q_1^2 \\ Q_2Q_7/Q_1 + 2Q_3Q_6/Q_1 - 2Q_2Q_3^2/Q_1^2 \\ Q_4Q_5/Q_1 + 2Q_2Q_8/Q_1 - 2Q_2^2Q_4/Q_1^2 \\ Q_4Q_6/{Q_1}^2 + Q_2Q_9/Q_1 + Q_3Q_8/Q_1 - 2Q_2Q_3Q_4/{Q_1}^2 \end{bmatrix}, \tag{2.37}$$

$$G_P = \begin{bmatrix} Q_3 \\ Q_6 \\ Q_7 \\ Q_9 \\ 2Q_2Q_6/Q_1 + Q_3Q_5/Q_1 - 2Q_2^2Q_3/Q_1 \\ Q_2Q_7/Q_1 + 2Q_3Q_6/Q_1 - 2Q_2Q_3^2/Q_1 \\ -2{Q_3}^3/{Q_1}^2 + 3Q_3Q_7/Q_1 \\ Q_4Q_6/{Q_1}^2 + Q_2Q_9/Q_1 + Q_3Q_8/Q_1 - 2Q_2Q_3Q_4/{Q_1}^2 \\ Q_4Q_7/Q_1 + 2Q_3Q_9/Q_1 - 2Q_3^2Q_4/Q_1^2 \end{bmatrix}. \tag{2.38}$$

Applying the chain rule, the characteristic form is derived,

$$\frac{\partial Q_P}{\partial t} + \frac{\partial F_P}{\partial Q_P}\frac{\partial Q_P}{\partial x} + \frac{\partial G_P}{\partial Q_P}\frac{\partial Q_P}{\partial y} = 0, \tag{2.39}$$

where $A_P = \frac{\partial F_P}{\partial Q_P}$ and $B_P = \frac{\partial G_P}{\partial Q_P}$ are the Jacobian matrix of the system in the x and y direction respectively,

$$A_p = \begin{bmatrix}
0 & 1 & 0 & 0 & 0 & 0 & 0 & 0 & 0 \\
0 & 0 & 0 & 0 & 1 & 0 & 0 & 0 & 0 \\
0 & 0 & 0 & 0 & 0 & 1 & 0 & 0 & 0 \\
0 & 0 & 0 & 0 & 0 & 0 & 0 & 1 & 0 \\
\widetilde{u_p}^2 - 3\sigma_{uu}\widetilde{u_p} & 3\sigma_{uu} - 3\widetilde{u_p}^2 & 0 & 0 & 3\widetilde{u_p} & 0 & 0 & 0 & 0 \\
\widetilde{v_p}\widetilde{u_p}^2 - 2\sigma_{uv}\widetilde{u_p} - \sigma_{uu}\widetilde{v_p} & 2\sigma_{uv} - 2\widetilde{u_p}\widetilde{v_p} & \sigma_{uu} - \widetilde{u_p}^2 & 0 & \widetilde{v_p} & 2\widetilde{u_p} & 0 & 0 & 0 \\
\widetilde{u_p}\widetilde{v_p}^2 - 2\sigma_{uv}\widetilde{v_p} - \sigma_{vv}\widetilde{u_p} & \sigma_{vv} - \widetilde{v_p}^2 & 2\sigma_{uv} - 2\widetilde{u_p}\widetilde{v_p} & 0 & 0 & 2\widetilde{v_p} & \widetilde{u_p} & 0 & 0 \\
\widetilde{\theta}\widetilde{u_p}^2 - 2qq_u\widetilde{u_p} - \sigma_{uu}\widetilde{\theta} & 2qq_u - 2\widetilde{\theta}\widetilde{u_p} & 0 & \sigma_{uu} - \widetilde{u_p}^2 & \widetilde{\theta} & 0 & 0 & 2\widetilde{u_p} & 0 \\
\widetilde{\theta}\widetilde{u_P}\widetilde{v_P} - qq_u\widetilde{v_p} - \sigma_{uv}\widetilde{\theta} - qq_v\widetilde{u_p} & qq_v - \widetilde{\theta}\widetilde{v_p} & qq_u - \widetilde{\theta}\widetilde{u_p} & \sigma_{uv} - \widetilde{u_p}\widetilde{v_p} & 0 & \widetilde{\theta} & 0 & \widetilde{v_p} & \widetilde{u_p}
\end{bmatrix}, \tag{2.40}$$

and the eigenvalues and eigenvectors associated,

$$\begin{aligned}
&\lambda_1 = \widetilde{u_P} - \sqrt{3\sigma_{uu}}, \quad \lambda_2 = \widetilde{u_P} + \sqrt{3\sigma_{uu}}, \\
&\lambda_3 = \widetilde{u_P}, \quad \lambda_4 = \widetilde{u_P}, \quad \lambda_5 = \widetilde{u_P}, \\
&\lambda_6 = \widetilde{u_P} + \sqrt{\sigma_{uu}}, \quad \lambda_7 = \widetilde{u_P} + \sqrt{\sigma_{uu}}, \\
&\lambda_8 = \widetilde{u_P} - \sqrt{\sigma_{uu}}, \quad \lambda_9 = \widetilde{u_P} - \sqrt{\sigma_{uu}},
\end{aligned}$$

$$r_1 = \begin{bmatrix}
1 \\
\widetilde{u_P} - \sqrt{3\sigma_{uu}} \\
\frac{\widetilde{v_P}\sqrt{\sigma_{uu}} - \sigma_{uv}\sqrt{3}}{\sqrt{\sigma_{uu}}} \\
\frac{\widetilde{\theta}\sqrt{\sigma_{uu}} - qq_u\sqrt{3}}{\sqrt{\sigma_{uu}}} \\
(\widetilde{u_P} - \sqrt{3\sigma_{uu}})^2 \\
\frac{(\widetilde{u_P} - \sqrt{3\sigma_{uu}})(\widetilde{v_P}\sqrt{\sigma_{uu}} - \sigma_{uv}\sqrt{3})}{\sqrt{\sigma_{uu}}} \\
\frac{\sigma_{uu}\sigma_{vv} + \sigma_{uu}\widetilde{v_P}^2 + 2\sigma_{uv}{}^2 - 2\widetilde{v_P}\sigma_{uv}\sqrt{3\sigma_{uu}}}{\sigma_{uu}} \\
\frac{(\widetilde{\theta}\sqrt{\sigma_{uu}} - qq_u\sqrt{3})(\widetilde{u_P} - \sqrt{3\sigma_{uu}})}{\sqrt{\sigma_{uu}}} \\
\frac{2qq_u\sigma_{uv} + qq_v\sigma_{uu} + \widetilde{v_P}\sigma_{uu}\widetilde{\theta} - qq_u\widetilde{v_P}\sqrt{3\sigma_{uu}} - \widetilde{\theta}\sigma_{uv}\sqrt{3\sigma_{uu}}}{\sigma_{uu}}
\end{bmatrix}, \tag{2.41}$$

$$r_2 = \begin{bmatrix} 1 \\ \widetilde{u_P} + \sqrt{3\sigma_{uu}} \\ \frac{\sigma_{uv}\sqrt{3}+\widetilde{v_P}\sqrt{\sigma_{uu}}}{\sqrt{\sigma_{uu}}} \\ \frac{qq_u\sqrt{3}+\widetilde{\theta}\sqrt{\sigma_{uu}}}{\sqrt{\sigma_{uu}}} \\ (\widetilde{u_P} + \sqrt{3\sigma_{uu}})^2 \\ \frac{(\widetilde{u_P}+\sqrt{3\sigma_{uu}})(\widetilde{v_P}\sqrt{\sigma_{uu}}+\sigma_{uv}\sqrt{3})}{\sqrt{\sigma_{uu}}} \\ \frac{\sigma_{uu}\sigma_{vv}+\sigma_{uu}\widetilde{v_P}^2+2{\sigma_{uv}}^2+2\widetilde{v_P}\sigma_{uv}\sqrt{3\sigma_{uu}}}{\sigma_{uu}} \\ \frac{(\widetilde{\theta}\sqrt{\sigma_{uu}}+qq_u\sqrt{3})(\widetilde{u_P}+\sqrt{3\sigma_{uu}})}{\sqrt{\sigma_{uu}}} \\ \frac{2qq_u\sigma_{uv}+qq_v\sigma_{uu}+\widetilde{v_P}\sigma_{uu}\widetilde{\theta}+qq_u\widetilde{v_P}\sqrt{3\sigma_{uu}}+\widetilde{\theta}\sigma_{uv}\sqrt{3\sigma_{uu}}}{\sigma_{uu}} \end{bmatrix}, \tag{2.42}$$

$$r_3 = \begin{bmatrix} 0 \\ 0 \\ 0 \\ 0 \\ 0 \\ 0 \\ 1 \\ 0 \\ 0 \end{bmatrix}, \quad r_4 = \begin{bmatrix} 1 \\ \widetilde{u_P} \\ \widetilde{v_P} \\ \widetilde{\theta} \\ \widetilde{u_P}^2 \\ \widetilde{u_P}\widetilde{v_P} \\ 0 \\ \widetilde{\theta}\widetilde{u_P} \\ 0 \end{bmatrix}, \quad r_5 = \begin{bmatrix} 0 \\ 0 \\ 0 \\ 0 \\ 0 \\ 0 \\ 0 \\ 0 \\ 1 \end{bmatrix}, \tag{2.43}$$

$$r_6 = \begin{bmatrix} 0 \\ 0 \\ 1 \\ \frac{-(qq_u+\widetilde{\theta}\sqrt{\sigma_{uu}})}{\sigma_{uv}+\widetilde{v_P}\sqrt{\sigma_{uu}}} \\ 0 \\ \widetilde{u_P} + \sqrt{\sigma_{uu}} \\ \frac{2(\sigma_{uv}+\widetilde{v_P}\sqrt{\sigma_{uu}})}{\sqrt{\sigma_{uu}}} \\ \frac{-(qq_u+\widetilde{\theta}\sqrt{\sigma_{uu}})(\widetilde{u_P}+\sqrt{\sigma_{uu}})}{\sigma_{uv}+\widetilde{v_P}\sqrt{\sigma_{uu}}} \\ 0 \end{bmatrix}, \quad r_7 = \begin{bmatrix} 0 \\ 0 \\ 1 \\ 0 \\ 0 \\ \widetilde{u_P} + \sqrt{\sigma_{uu}} \\ \frac{2(\sigma_{uv}+\widetilde{v_P}\sqrt{\sigma_{uu}})}{\sqrt{\sigma_{uu}}} \\ 0 \\ \frac{qq_u+\widetilde{\theta}\sqrt{\sigma_{uu}}}{\sqrt{\sigma_{uu}}} \end{bmatrix}, \tag{2.44}$$

$$r_8 = \begin{bmatrix} 0 \\ 0 \\ 1 \\ \frac{-(qq_u-\widetilde{\theta}\sqrt{\sigma_{uu}})}{\sigma_{uv}+\widetilde{v_P}\sqrt{\sigma_{uu}}} \\ 0 \\ \widetilde{u_P} - \sqrt{\sigma_{uu}} \\ \frac{-2(\sigma_{uv}-\widetilde{v_P}\sqrt{\sigma_{uu}})}{\sqrt{\sigma_{uu}}} \\ \frac{-(qq_u-\widetilde{\theta}\sqrt{\sigma_{uu}})(\widetilde{u_P}-\sqrt{\sigma_{uu}})}{\sigma_{uv}-\widetilde{v_P}\sqrt{\sigma_{uu}}} \\ 0 \end{bmatrix}, \quad r_9 = \begin{bmatrix} 0 \\ 0 \\ 1 \\ 0 \\ 0 \\ \widetilde{u_P} - \sqrt{\sigma_{uu}} \\ \frac{-2(\sigma_{uv}-\widetilde{v_P}\sqrt{\sigma_{uu}})}{\sqrt{\sigma_{uu}}} \\ 0 \\ \frac{-(qq_u-\widetilde{\theta}\sqrt{\sigma_{uu}})}{\sqrt{\sigma_{uu}}} \end{bmatrix}. \tag{2.45}$$

In y direction,

$$B_p = \begin{bmatrix} 0 & 0 & 1 & 0 & 0 & 0 & 0 & 0 & 0 \\ 0 & 0 & 0 & 0 & 0 & 1 & 0 & 0 & 0 \\ 0 & 0 & 0 & 0 & 0 & 0 & 1 & 0 & 0 \\ 0 & 0 & 0 & 0 & 0 & 0 & 0 & 0 & 1 \\ \widetilde{v_p}\widetilde{u_p}^2 - 2\sigma_{uv}\widetilde{u_p} - \sigma_{uu}\widetilde{v_p} & 2\sigma_{uv} - 2\widetilde{u_p}\widetilde{v_p} & \sigma_{uu} - \widetilde{u_p}^2 & 0 & \widetilde{v_p} & 2\widetilde{u_p} & 0 & 0 & 0 \\ \widetilde{u_p}\widetilde{v_p}^2 - 2\sigma_{uv}\widetilde{v_p} - \sigma_{vv}\widetilde{u_p} & \sigma_{vv} - \widetilde{v_p}^2 & 2\sigma_{uv} - 2\widetilde{u_p}\widetilde{v_p} & 0 & 0 & 2\widetilde{v_p} & \widetilde{u_p} & 0 & 0 \\ \widetilde{v_p}^3 - 3\sigma_{vv}\widetilde{v_p} & 0 & 3\sigma_{vv} - 3\widetilde{v_p}^2 & 0 & 0 & 0 & 3\widetilde{v_p} & 0 & 0 \\ \widetilde{\theta}\widetilde{u_p}\widetilde{v_p} - qq_u\widetilde{v_p} - \sigma_{uv}\widetilde{\theta} - qq_v\widetilde{u_p} & qq_v - \widetilde{\theta}\widetilde{v_p} & qq_u - \widetilde{\theta}\widetilde{u_p} & \sigma_{uv} - \widetilde{u_p}\widetilde{v_p}^2 & 0 & \widetilde{\theta} & 0 & \widetilde{v_p} & \widetilde{u_p} \\ \widetilde{\theta}\widetilde{v_p}^2 - 2qq_v\widetilde{v_p} - \sigma_{vv}\widetilde{\theta} & 0 & 2qq_v - 2\widetilde{\theta}\widetilde{v_p} & \sigma_{vv} - \widetilde{v_p}^2 & 0 & 0 & \widetilde{\theta} & 0 & 2\widetilde{v_p} \end{bmatrix}, \tag{2.46}$$

and the eigenvalues and eigenvectors associated,

$\lambda_1 = \widetilde{v_P} - \sqrt{3\sigma_{vv}}, \quad \lambda_2 = \widetilde{v_P} + \sqrt{3\sigma_{vv}},$
$\lambda_3 = \widetilde{v_P}, \quad \lambda_4 = \widetilde{v_P}, \quad \lambda_5 = \widetilde{v_P},$
$\lambda_6 = \widetilde{v_P} + \sqrt{\sigma_{vv}}, \quad \lambda_7 = \widetilde{v_P} + \sqrt{\sigma_{vv}},$
$\lambda_8 = \widetilde{v_P} - \sqrt{\sigma_{vv}}, \quad \lambda_9 = \widetilde{v_P} - \sqrt{\sigma_{vv}},$

$$r_1 = \begin{bmatrix} 1 \\ \frac{\widetilde{u_P}\sqrt{\sigma_{vv}} - \sigma_{uv}\sqrt{3}}{\sqrt{\sigma_{vv}}} \\ \widetilde{v_P} - \sqrt{3\sigma_{vv}} \\ \frac{\widetilde{\theta}\sqrt{\sigma_{vv}} - qq_v\sqrt{3}}{\sqrt{\sigma_{vv}}} \\ \frac{\sigma_{uu}\sigma_{vv} + \sigma_{vv}\widetilde{u_P}^2 + 2\sigma_{uv}{}^2 - 2\widetilde{u_P}\sigma_{uv}\sqrt{3\sigma_{vv}}}{\sigma_{vv}} \\ \frac{(\widetilde{v_P} - \sqrt{3\sigma_{vv}})(\widetilde{u_P}\sqrt{\sigma_{vv}} - \sigma_{uv}\sqrt{3})}{\sqrt{\sigma_{vv}}} \\ (\widetilde{v_P} - \sqrt{3\sigma_{vv}})^2 \\ \frac{2qq_v\sigma_{uv} + qq_u\sigma_{vv} + \widetilde{u_P}\sigma_{vv}\widetilde{\theta} - qq_v\widetilde{u_P}\sqrt{3\sigma_{vv}} - \widetilde{\theta}\sigma_{uv}\sqrt{3\sigma_{vv}}}{\sigma_{vv}} \\ \frac{(\widetilde{\theta}\sqrt{\sigma_{vv}} - qq_v\sqrt{3})(\widetilde{v_P} - \sqrt{3\sigma_{vv}})}{\sqrt{\sigma_{vv}}} \end{bmatrix}, \tag{2.47}$$

$$r_2 = \begin{bmatrix} 1 \\ \frac{\sigma_{uv}\sqrt{3} + \widetilde{u_P}\sqrt{\sigma_{vv}}}{\sqrt{\sigma_{vv}}} \\ \widetilde{v_P} + \sqrt{3\sigma_{vv}} \\ \frac{qq_v\sqrt{3} + \widetilde{\theta}\sqrt{\sigma_{vv}}}{\sqrt{\sigma_{vv}}} \\ \frac{\sigma_{uu}\sigma_{vv} + \sigma_{vv}\widetilde{u_P}^2 + 2\sigma_{uv}{}^2 + 2\widetilde{u_P}\sigma_{uv}\sqrt{3\sigma_{vv}}}{\sigma_{vv}} \\ \frac{(\widetilde{v_P} + \sqrt{3\sigma_{vv}})(\widetilde{u_P}\sqrt{\sigma_{vv}} + \sigma_{uv}\sqrt{3})}{\sqrt{\sigma_{vv}}} \\ (\widetilde{v_P} + \sqrt{3\sigma_{vv}})^2 \\ \frac{2qq_v\sigma_{uv} + qq_u\sigma_{vv} + \widetilde{u_P}\sigma_{vv}\widetilde{\theta} + qq_v\widetilde{u_P}\sqrt{3\sigma_{vv}} + \widetilde{\theta}\sigma_{uv}\sqrt{3\sigma_{vv}}}{\sigma_{vv}} \\ \frac{(\widetilde{\theta}\sqrt{\sigma_{vv}} + qq_v\sqrt{3})(\widetilde{v_P} + \sqrt{3\sigma_{vv}})}{\sqrt{\sigma_{vv}}} \end{bmatrix}, \tag{2.48}$$

$$r_3 = \begin{bmatrix} 0 \\ 0 \\ 0 \\ 0 \\ 1 \\ 0 \\ 0 \\ 0 \\ 0 \end{bmatrix}, \quad r_4 = \begin{bmatrix} 1 \\ \widetilde{u_P} \\ \widetilde{v_P} \\ \widetilde{\theta} \\ 0 \\ \widetilde{u_P}\widetilde{v_P} \\ \widetilde{v_P}^2 \\ 0 \\ \widetilde{\theta}\widetilde{v_P} \end{bmatrix}, \quad r_5 = \begin{bmatrix} 0 \\ 0 \\ 0 \\ 0 \\ 0 \\ 0 \\ 0 \\ 1 \\ 0 \end{bmatrix}, \tag{2.49}$$

$$r_6 = \begin{bmatrix} 0 \\ 1 \\ 0 \\ \frac{-(qq_v+\widetilde{\theta}\sqrt{\sigma_{vv}})}{\sigma_{uv}+\widetilde{u_P}\sqrt{\sigma_{vv}}} \\ \frac{2(\sigma_{uv}+\widetilde{u_P}\sqrt{\sigma_{vv}})}{\sqrt{\sigma_{vv}}} \\ \widetilde{v_P}+\sqrt{\sigma_{vv}} \\ 0 \\ 0 \\ \frac{-(qq_v+\widetilde{\theta}\sqrt{\sigma_{vv}})(\widetilde{v_P}+\sqrt{\sigma_{vv}})}{\sigma_{uv}+\widetilde{u_P}\sqrt{\sigma_{vv}}} \end{bmatrix}, \quad r_7 = \begin{bmatrix} 0 \\ 1 \\ 0 \\ 0 \\ \frac{2(\sigma_{uv}+\widetilde{u_P}\sqrt{\sigma_{vv}})}{\sqrt{\sigma_{vv}}} \\ \widetilde{v_P}+\sqrt{\sigma_{vv}} \\ 0 \\ \frac{qq_v+\widetilde{\theta}\sqrt{\sigma_{vv}}}{\sqrt{\sigma_{vv}}} \\ 0 \end{bmatrix}, \tag{2.50}$$

$$r_8 = \begin{bmatrix} 0 \\ 1 \\ 0 \\ \frac{-(qq_v-\widetilde{\theta}\sqrt{\sigma_{vv}})}{\sigma_{uv}+\widetilde{u_P}\sqrt{\sigma_{vv}}} \\ \frac{-2(\sigma_{uv}-\widetilde{u_P}\sqrt{\sigma_{vv}})}{\sqrt{\sigma_{vv}}} \\ \widetilde{v_P}-\sqrt{\sigma_{vv}} \\ 0 \\ 0 \\ \frac{-(qq_v-\widetilde{\theta}\sqrt{\sigma_{vv}})(\widetilde{v_P}-\sqrt{\sigma_{vv}})}{\sigma_{uv}-\widetilde{u_P}\sqrt{\sigma_{vv}}} \end{bmatrix}, \quad r_9 = \begin{bmatrix} 0 \\ 1 \\ 0 \\ 0 \\ \frac{-2(\sigma_{uv}-\widetilde{u_P}\sqrt{\sigma_{vv}})}{\sqrt{\sigma_{vv}}} \\ \widetilde{v_P}-\sqrt{\sigma_{vv}} \\ 0 \\ \frac{-(qq_v-\widetilde{\theta}\sqrt{\sigma_{vv}})}{\sqrt{\sigma_{vv}}} \\ 0 \end{bmatrix}. \tag{2.51}$$

2.3 Two-Way Coupling

We couple the phases by including a Source Term which accounts for the interaction between the Carrier Phase and the Disperse Phase in the Fluid governing equations as well as in the Particle governing equations. A momentum and energy tansfer occurs between the phases. Because we are working with immiscible fluids, no mass transfer is observed. The fluid source terms are,

$$S_f = \begin{bmatrix} 0 \\ \frac{m_P\widetilde{\phi}}{\tau_P}(\widetilde{u_P} - u) \\ \frac{m_P\widetilde{\phi}}{\tau_P}(\widetilde{v_P} - v) \\ \frac{\beta m_P\widetilde{\phi}}{(\gamma-1)M_f^2\tau_T}(\widetilde{\theta} - T) + \frac{m_P\widetilde{\phi}}{\tau_P}(\sigma_{uu} + \widetilde{u_P}^2 + \widetilde{u_P}u) \quad + \frac{m_P\widetilde{\phi}}{\tau_P}(\sigma_{vv} + \widetilde{v_P}^2 + \widetilde{v_P}v) \end{bmatrix}, \tag{2.52}$$

and particle source terms are,

$$S_P = \begin{bmatrix} 0 \\ \frac{\widetilde{\phi}}{\tau_P}(u - \widetilde{u_P}) \\ \frac{\widetilde{\phi}}{\tau_P}(v - \widetilde{v_P}) \\ \frac{\widetilde{\phi}}{\tau_T}(T - \widetilde{\theta}) \\ \frac{\widetilde{\phi}}{\tau_P}(\widetilde{u_P}^2 - \widetilde{u_P}u + \sigma_{uu}) \\ -\frac{\widetilde{\phi}}{\tau_P}(2\sigma_{uv} - u\widetilde{v_P} - v\widetilde{u_P} + 2\widetilde{u_P}\widetilde{v_P}) \\ \frac{\widetilde{\phi}}{\tau_P}(\widetilde{v_P}^2 - \widetilde{v_P}v + \sigma_{vv}) \\ -\frac{\widetilde{\phi}}{\tau_P}(qq_u - T\widetilde{u_P} + \widetilde{\theta}\widetilde{u_P} + \widetilde{\theta}\widetilde{v_P}) - \frac{\widetilde{\phi}}{\tau_P}(qq_u - \widetilde{\theta}u + \widetilde{\theta}\widetilde{u_P} + \widetilde{\theta}\widetilde{v_P}) \\ -\frac{\widetilde{\phi}}{\tau_T}(qq_v - T\widetilde{v_P} + \widetilde{\theta}\widetilde{u_P} + \widetilde{\theta}\widetilde{v_P}) - \frac{\widetilde{\phi}}{\tau_P}(qq_v - \widetilde{\theta}v + \widetilde{\theta}\widetilde{u_P} + \widetilde{\theta}\widetilde{v_P}) \end{bmatrix}. \tag{2.53}$$

The fully-coupled E-E model can be written as ,

$$\frac{\partial Q_f}{\partial t} + \frac{\partial F_f}{\partial x} + \frac{\partial G_f}{\partial y} = S_f, \tag{2.54}$$

$$\frac{\partial Q_P}{\partial t} + \frac{\partial F_P}{\partial x} + \frac{\partial G_P}{\partial y} = S_P. \tag{2.55}$$

Chapter 3

Numerical Methods

3.1 Averaging

The first step in discretizing the governing equations is to linearize the non-linear Jacobian matrix of the hyperbolic problem. Roe Averaging is used in the Eulerian phase over the primitive variables to obtain a linear Jacobian:

$$\hat{u}_{i-\frac{1}{2}} = \frac{\sqrt{\rho_{i-1}}u_{i-1} + \sqrt{\rho_i}u_i}{\sqrt{\rho_{i-1}} + \sqrt{\rho_i}}, \tag{3.1}$$

$$\hat{v}_{i-\frac{1}{2}} = \frac{\sqrt{\rho_{i-1}}v_{i-1} + \sqrt{\rho_i}v_i}{\sqrt{\rho_{i-1}} + \sqrt{\rho_i}}, \tag{3.2}$$

$$\hat{H}_{i-\frac{1}{2}} = \frac{\sqrt{\rho_{i-1}}H_{i-1} + \sqrt{\rho_i}H_i}{\sqrt{\rho_{i-1}} + \sqrt{\rho_i}} = \frac{(E_{i-1} + p_{i-1})/\sqrt{\rho_{i-1}} + (E_i + p_i)/\sqrt{\rho_i}}{\sqrt{\rho_{i-1}} + \sqrt{\rho_i}}, \tag{3.3}$$

$$\hat{c} = \sqrt{(\gamma - 1)(\hat{H} - \frac{1}{2}\hat{u}^2)}. \tag{3.4}$$

Where u_{i-1} is the velocity in x evaluated in the cell before, u_i is the velocity in x evaluated in the cell after and $\hat{u}_{i-\frac{1}{2}}$ is the averaged velocity in x, evaluated in the cell boundaries between the two cells previously cited. The same occurs for the other variables.
Simple Averaging is used in the Particle Phase,

$$\hat{q}_{i-\frac{1}{2}} = \frac{1}{2}(q_{i-1} + q_i), \tag{3.5}$$

where $\hat{q}_{i-\frac{1}{2}}$ represents the primitive variables $\widetilde{\phi}$, $\widetilde{u_p}$, $\widetilde{v_p}$, $\widetilde{\theta}$, $\widetilde{u_p}^2$, $\widetilde{u_p v_p}$, $\widetilde{v_p}^2$, $\widetilde{\theta u_p}$, $\widetilde{\theta v_p}$ explained in Chapter 2 and evaluated in the cell boundary.

3.2 WENO method

A Weight Esentially Non Oscillatory Conservative Finite Difference Scheme (WENO Scheme) is suitable for this problem because it provides high accuracy in smooth areas, good resolution around discontinuities and the necessary dissipation for shock capturing. More information about WENO scheme is provided by [3] and [4].

An uniform grid is defined by the points $x_i = i\Delta x$, i=0,...,N, called cell centers and the cell boundaries are given by $x_{i+\frac{1}{2}} = x_i + \frac{\Delta x}{2}$ where Δx is the uniform grid spacing.

The discretization yields a system of ordinary differential equations,

$$\frac{du_i(t)}{dt} = -\frac{\partial f}{\partial x}\Big|_{x=x_i} \quad i = 0, ..., N, \tag{3.6}$$

where $u_i(t)$ is the numercial approximation to the point value $u(x_i, t)$. We define the numerical flux function as $h(x)$. The conservative property of the spatial discretization is obtained by this function,

$$f(x) = \frac{1}{\Delta x}\int_{x-\Delta x}^{x+\Delta x} h(\xi)d\xi, \tag{3.7}$$

and the spatial derivative in 3.6 is expressed by a conservative finite-difference formula in the cell boundaries,

$$\frac{du_i(t)}{dt} = \frac{1}{\Delta x}(h_{i+\frac{1}{2}} - h_{i-\frac{1}{2}}) \tag{3.8}$$

A high order polinomial interpolation over $h(x)$, using the known values of f in x_i, is used to determine this formula. The fifth order WENO scheme uses a 5 points stencil, S_5, composed of three 3-points stencil, S_0, S_1, S_2, shown in Fig. 3.1. The fifth order approximation $\hat{f}_{i\pm\frac{1}{2}}$ is built through a convex combination of the interpolated values $\hat{f}_{i\pm\frac{1}{2}}$,

$$\hat{f}_{i\pm\frac{1}{2}} = \sum_{k=0}^{2} \omega_k^z \hat{f}^k(x_i \pm \frac{1}{2}), \tag{3.9}$$

where

$$\hat{f}^k_{i\pm\frac{1}{2}} = \sum_{k=0}^{2} c_{kj} f_{i-k+j}, \quad i = 0, ..., N, \tag{3.10}$$

and c_{kj} are the Lagrangian interpolation coefficients, which depend on the parameter k. This convex combination is made by weighing the different solutions obtained with the sub-stencils. The WENO weights are defined as

$$\omega_k^z = \frac{\alpha_k^z}{\sum_{l=0}^{2}\alpha_k^z}, \quad \omega_k^z = \frac{d_k}{\beta_k^z}, \quad k = 0, 1, 2, \tag{3.11}$$

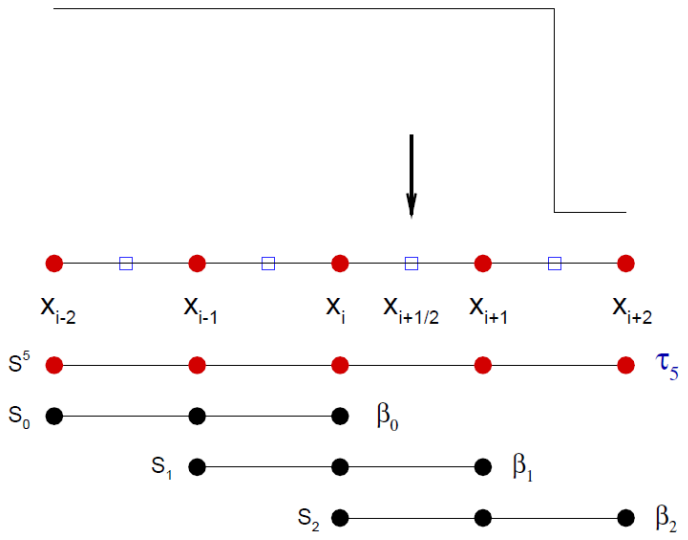

FIGURE 3.1: Discontinuity between cell boundaries x_{i+1} and x_{i+2}. $x_{i+1/2}$ represents a cell center. WENO scheme 5-points Stencil is S_5. Three 3-points substencil are (S_0, S_1, S_2).

where $d_0 = \frac{3}{10}$, $d_1 = \frac{3}{5}$, $d_2 = \frac{1}{10}$ are the ideal weights and they generate a central upwind fifth order scheme for the 5-points stencil. The weights are also a function of the smoothness indicator given by β_k, which measures the regularity of the k^{th} polynomial approximation.

If the smoothness indicators are close to one, the substencil weights are close to the ideal weights. However, if S_k contains a discontinuity, β_k is $O(1)$ and the corresponding weight, ω_k, is relatively small compared with the other weights. Because of the lower weighting, the influence of the polynomial approximation of $h_{i\pm\frac{1}{2}}$ taken across the discontinuity is dismished in the global solution up to the point, making the scheme effectively lower order near the discontinuity and esentially preventing oscillations.

3.3 Temporal Stability

The Courant-Friedrichs-Lewy condition, CFL condition is necessary in order to assure the stability and convergence of the method,

$$\Delta t = \quad CFL * \frac{min(\Delta x, \Delta y)}{max(\lambda_x^f \lambda_y^f)}, \tag{3.12}$$

where Δt is the time step, λ are the eigenvalues of the carrier phase in the x and y dimensions and $\Delta x, \Delta y$ are the uniform grid spacing in the x and y dimensions respectively. A RK3 scheme is used to update the time step so we obtain more stability than a first-order scheme and there is no need to split dimensionally.

Chapter 4

Moving Normal Shockwave

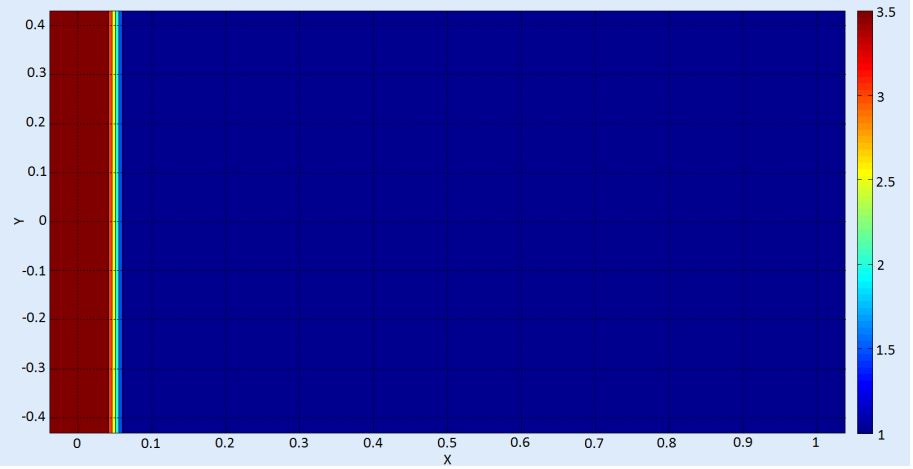

FIGURE 4.1: Carrier Phase Setup

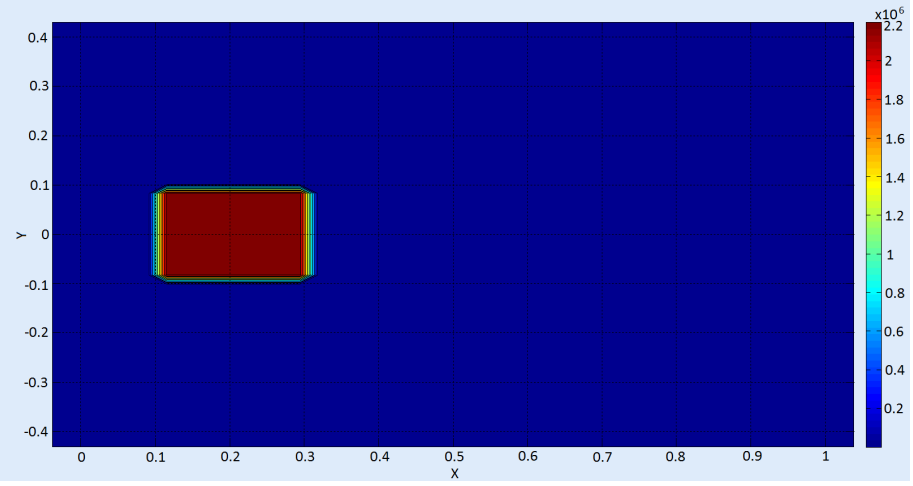

FIGURE 4.2: Particle Phase Setup

4.1 Setup

We consider two-dimensional case of a moving shock at $M = 3.0$ initialized at $x_s = 0.05$ in a rectangular domain of $[0, 1.0] * [-0.4, 0.4]$, interacting with a rectangular particle cloud at zero velocity, with 90,000 particles uniformly distributed of $[0.1, 0.3]x[-0.1, 0.1]$. The density of each particle is $\rho_p = 1000$, the diameter is $d = 5.86 * 10^{-3}$. Particles are initially in energy equilibrium. Fluid velocity downstram is initially set to zero.

x_0	x_1	y_0	y_1	xP_0	xP_1	yP_0	yP_1
0.0	1.0	-0.4	0.4	0.1	0.3	-0.1	0.1

TABLE 4.1: Domain setup.

Mach	γ	β	St	ρ	p	u	v	x_s
3.0	1.4	0.4	0.4	1.0	1.0	0.0	0.0	0.05

TABLE 4.2: Carrier Phase initial conditions.

N_p	M_p	ϕ	u_p	v_p	θ	σ_{uu}	σ_{uv}	σ_{vv}	qq_u	qq_v
90,000	1.055e-4	2.25e6	0.0	0.0	T_f	eps	eps	eps	0.0	0.0

TABLE 4.3: Disperse Phase initial conditions.

Boundary Conditions Expanding shockwave

4.2 Results

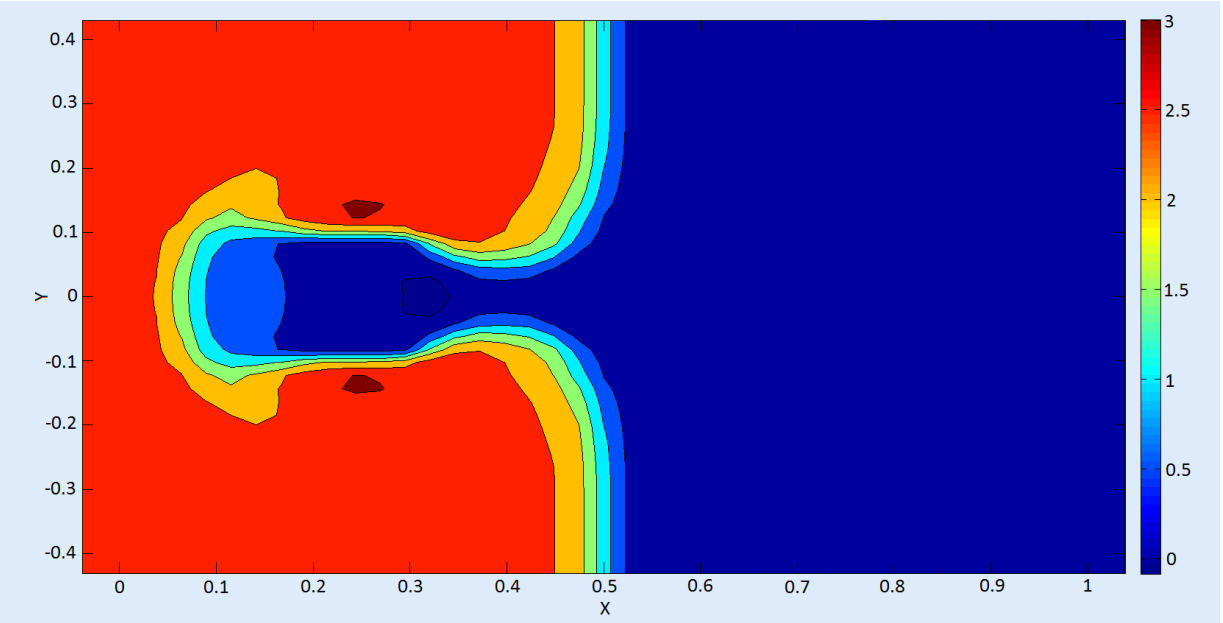

FIGURE 4.3: Fluid velocity in x direction, at the time 0.14s

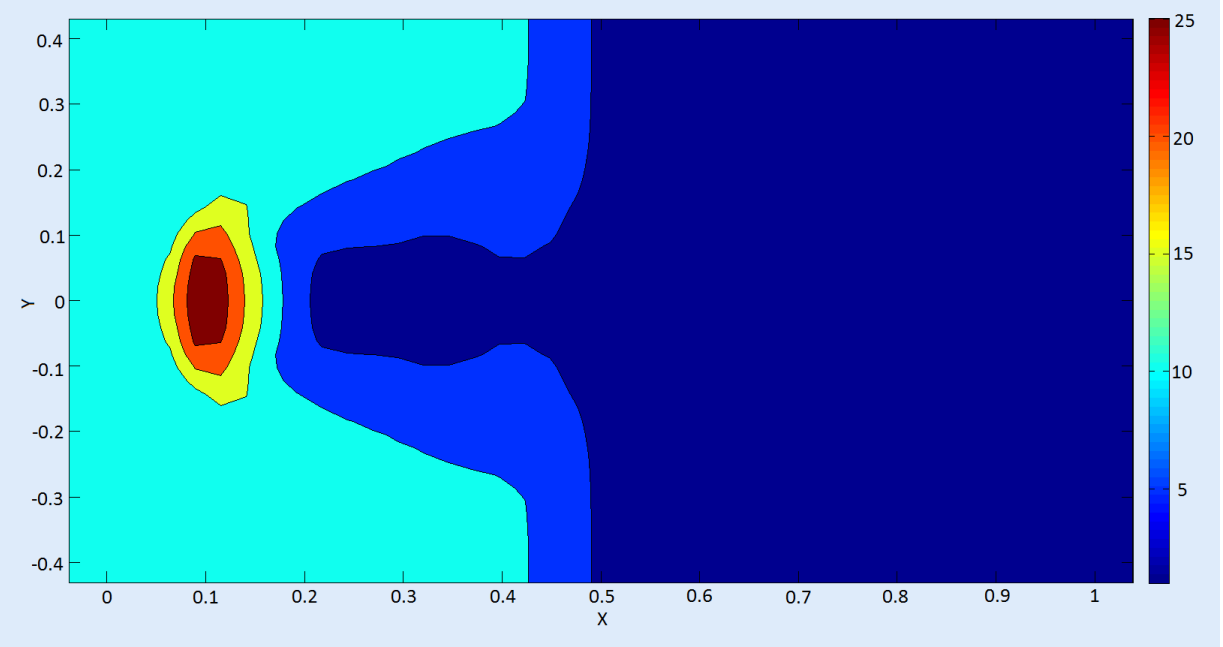

FIGURE 4.4: Fluid pressure, at the time 0.14s

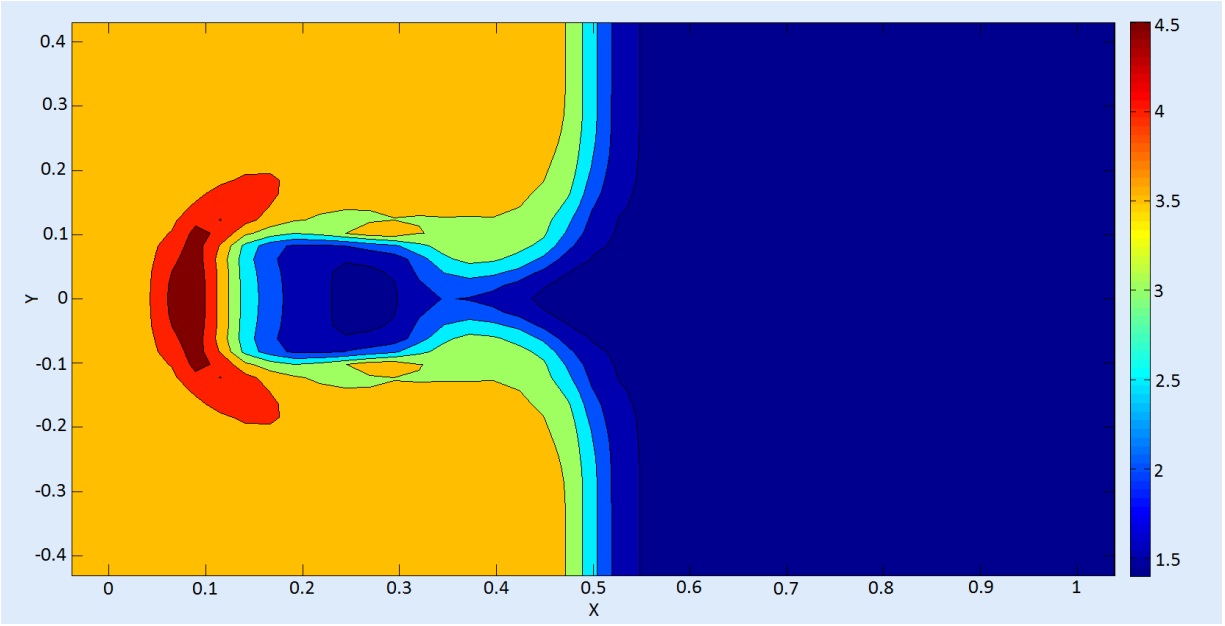

FIGURE 4.5: Fluid temperature, at the time 0.14s

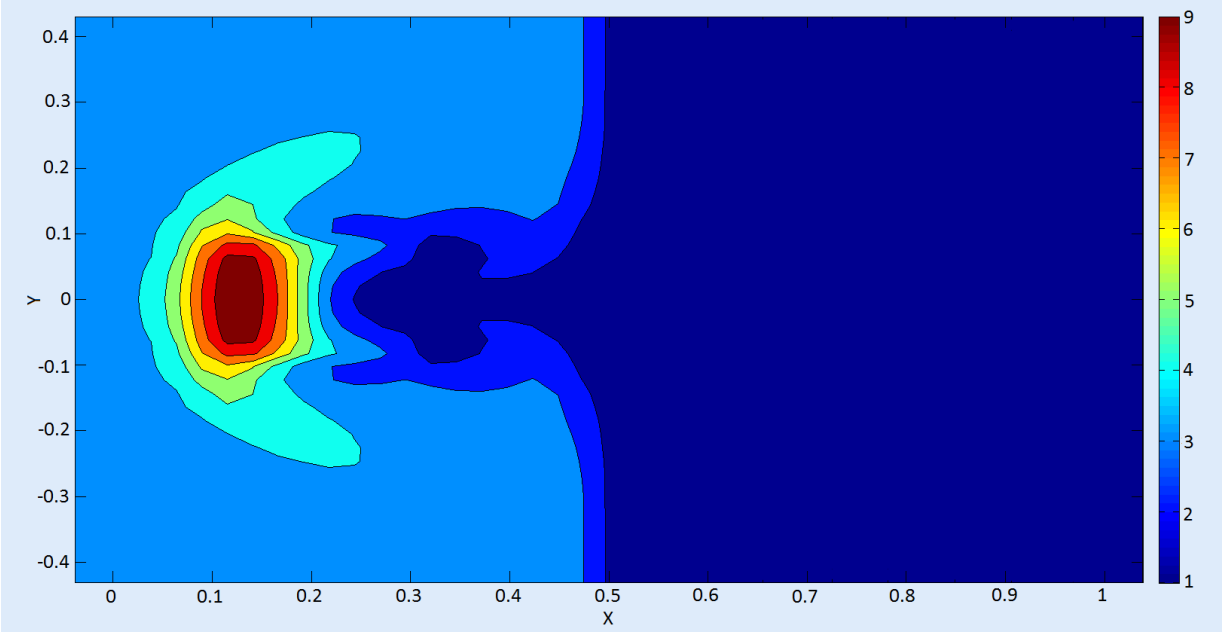

FIGURE 4.6: Fluid density, at the time 0.14s

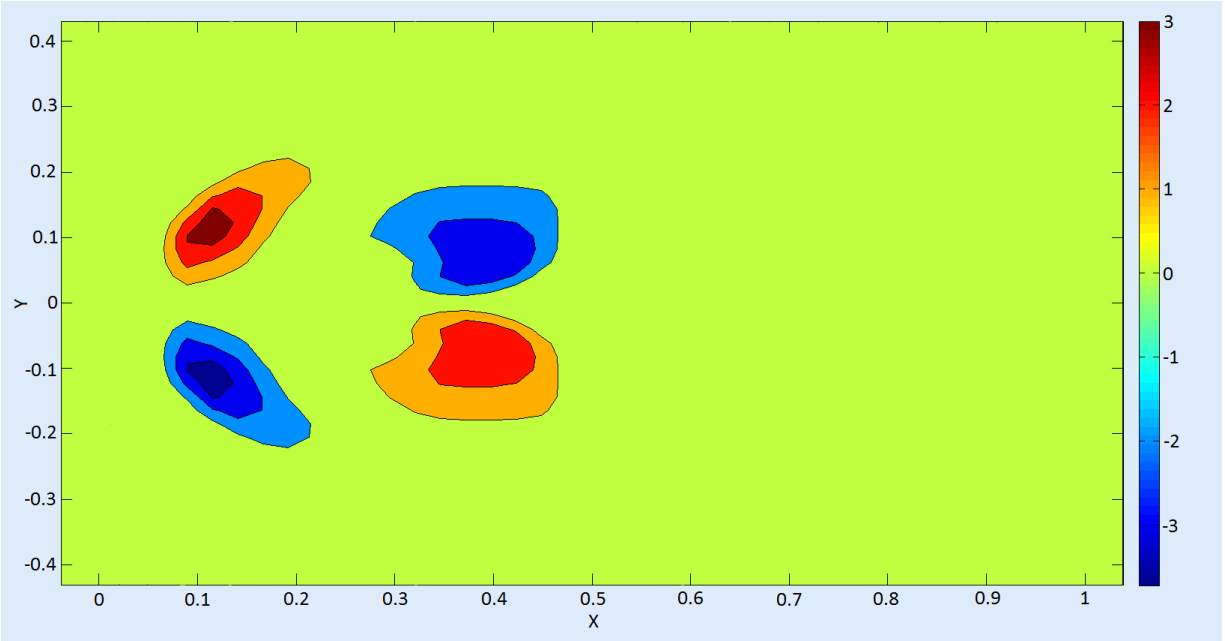

FIGURE 4.7: Fluid velocity in y direction, at the time 0.14s

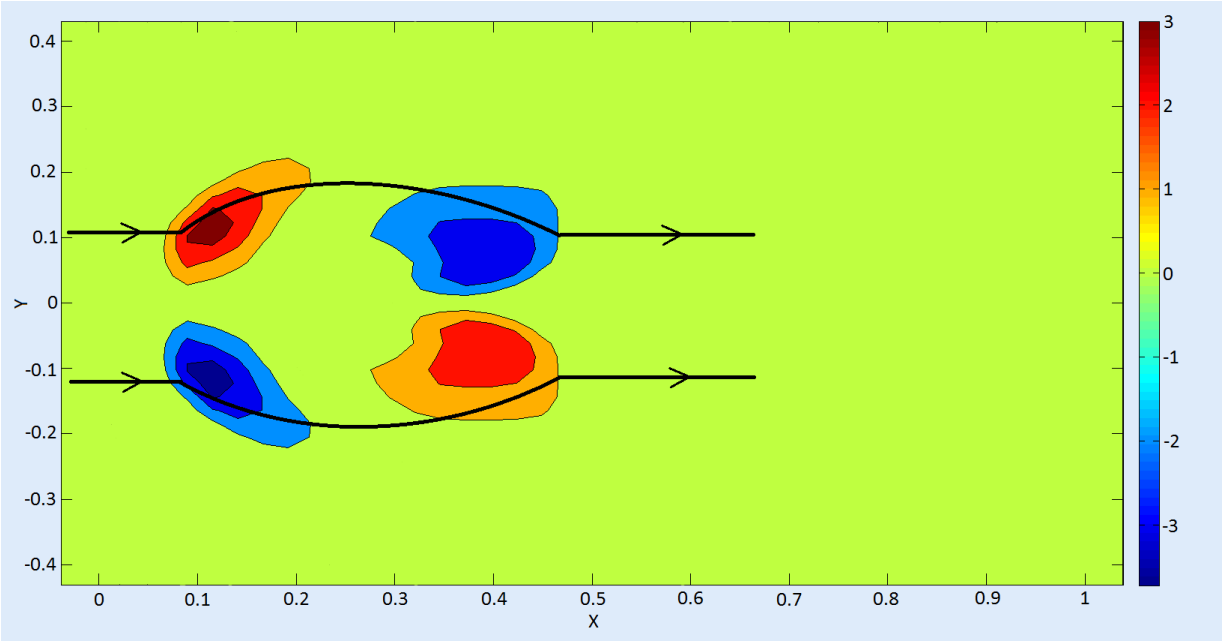

FIGURE 4.8: Streamlines around the particle cloud, at the time 0.14s

4.2.1 Carrier Phase

The flow behind the Shockwave is supersonic and has the same Mach number as the shockwave while the upstream flow is at rest. Across the normal shock, the velocity decreases instantaneously to subsonic values, while the pressure, density and temperature increase. As it is seen; by the moment the problem is analyzed, the shock is at $x = 0.5$ As the shock moves downstream and interacts with the cloud of particles, a bow shock forms upstream of the cloud. This bow shock is called the induced shock to differenciate it from the initial shock. The flow deccelerates across the induced shock, causing a decrease in the kinetic energy of the carrier phase, (figure 4.3). Because no energy is generated in the system, an increase in the internal and static energy of the flow compensates for the decrease in kinetic energy as shown in figures 4.4 and 4.5. Following the ideal gas law, the increased static energy results in an increase of the fluid density, figure 4.6.

After the induced schock, the flow interacts with the particles causing a gradual decrease in the velocity, pressure and temperature. The decreased velocity, pressure and temperature occur because of the energy and momentum transfer from the fluid to the particle phase, while the increased density is due to the slowing of the fluid. The particles are initiallized with zero velocity and in energy equilibrium with the Carrier Phase.

Figure 4.7 shows the velocity in y and in Figure 4.8 is shown the streamlines through the particle cloud.

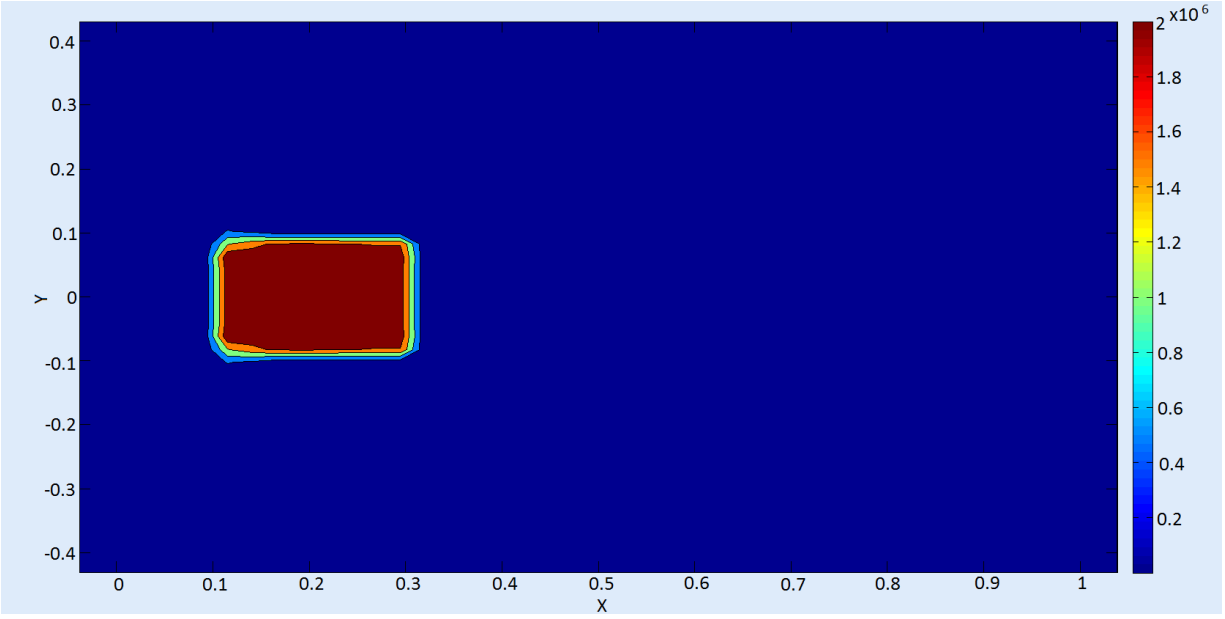

FIGURE 4.9: Particle density number, at the time 0.14s

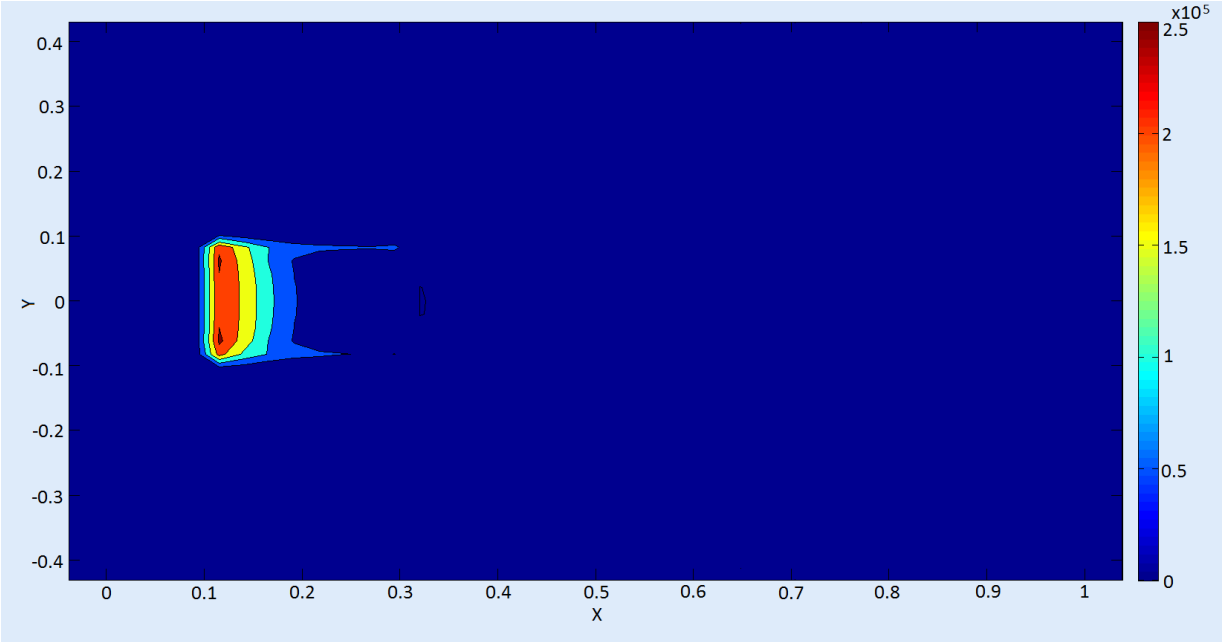

FIGURE 4.10: Particle velocity in x direction, at the time 0.14s

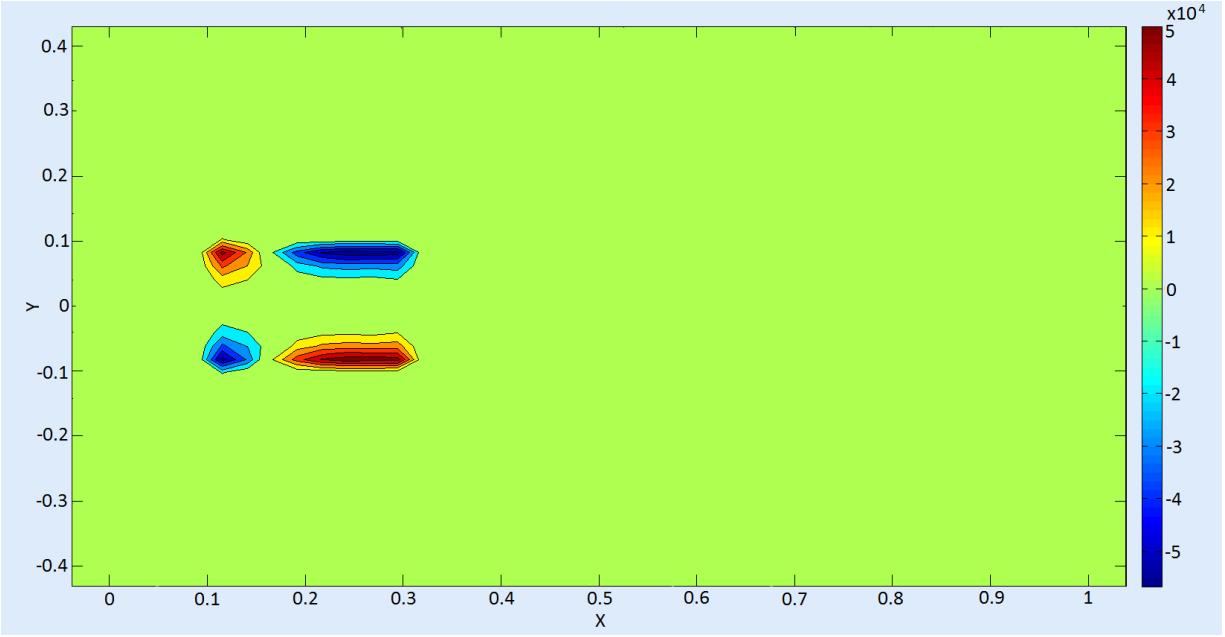

FIGURE 4.11: Particle velocity in y direction, at the time 0.14s

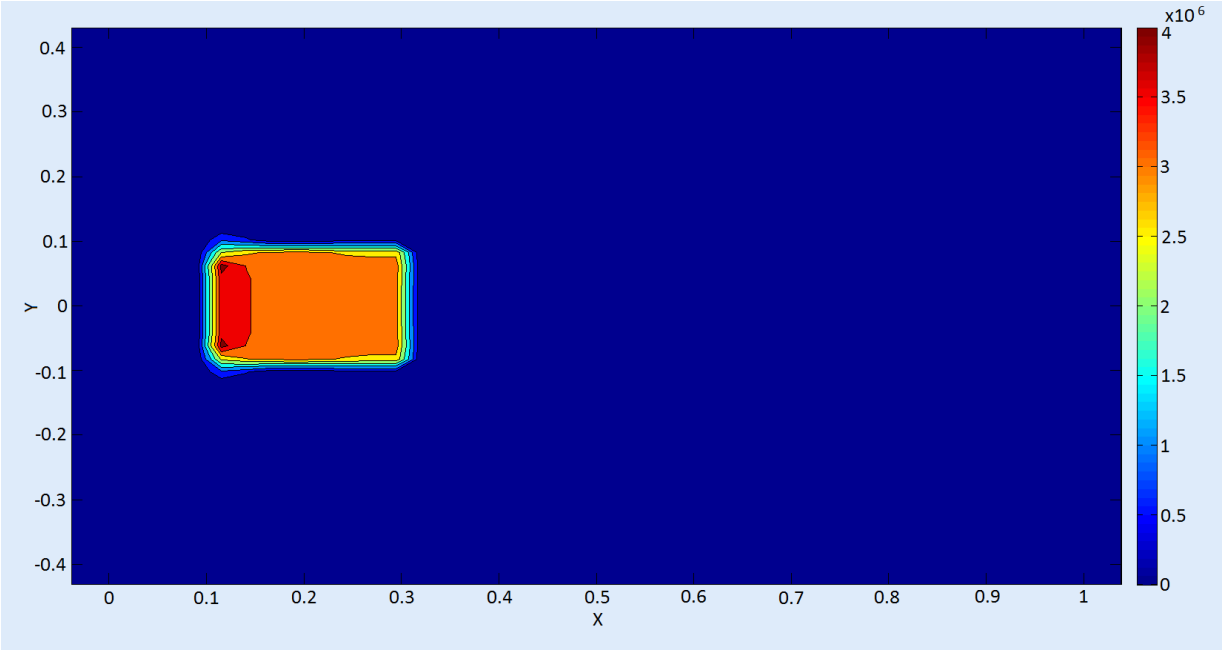

FIGURE 4.12: Particle temperature, at the time 0.14s

4.2.2 Disperse Phase

When the flow passes through the particle cloud, this experiments a decrease in the kinetic, static and internal energy. The particles initially at the leading edge start accelerating and overtaking the particles initially at the rear of the cloud. At later times, more particles are accelerated due to the flow or pushed by other particles, hence the cloud moves forward.

In figure 4.12, particle temperature is shown. The particles in the leading edge experiment a larger increase of temperature because the temperature of the fluid in this area is higher. The particle velocity in y presents a similar behaviour owing to the coupling and momentum transfer between phases. Particles in the leading edge of the cloud are pushed out of the cloud so these particles wil be spread away, while particles in the trailing edge of the cloud are pushed into the cloud. This will mean that the cloud of particles will be narrower and longer in the trailing edge but shorter and wider in the leading edge of the cloud at later times.

Chapter 5

Conclusions and Future Work

A 2D Eulerian Eulerian model is presented to compute a two-way coupled particle laden flow in a compressible fluid. The EE model couples the inviscid Euler equations with a new set of Eulerian equations developed for the particle phase, derived with a filtered Liouville equation that governs the particle density function. Second moments of the particle phase result in a non-linear system of equatios while third moments are simplified by asumming third order correlations are neglegible.

To linearize the problem, a Roe averaging scheme is used in the carrier phase and simple averaging is used in the disperse phase. The model is discretized using a uniform grid and fluxes are computed with a high order Weight Esentially Non-Oscillatory conservative finite difference scheme, also known as high order WENO scheme. WENO methods have high accuracy in smooth areas while providing good resolution around discontinuities as well as the neccessary dissipation for shock capturing. In order to assure the stability and convergence of the method, a CFL condition is used to modulate the time step. Finally, time is updated with a RK3 scheme.

The interaction of a right-running normal shock and an initially stationary and in energy equilibrium rectangular cloud of particles, is analyzed. Fluid is supersonic upstream and subsonic downstream. The only mechanism that a supersonic flow has to adapt to an obstacle like the cloud of particles is, is by a bow shock, also called induced shock. This shock makes the velocity decrease to subsonic values and the pressure and termperature increase. Following the ideal gas law, result in an increase of the density.

As the shock runs through the cloud of particles, fluid phase transfer energy and momentum to the particle phase, increasing the temperature of the particles at the leading edge of the cloud while this particles start to accelerate downstream. The cloud is an obstacle for the flow so the streamlines surround the cloud and this generates in the flow

a velocity in y. This velocity is also transferred to the particles making the cloud not only move down stream but also change its initially rectangular shape.

Future lines would focus on comparing different ways to solve the problem since the EE approach using a different scheme such us Godunov based schemes or high order upwind schemes. Other future efforts could focus on compared the results between the EE and EL approaches using a WENO scheme.

Bibliography

[1] Truong, Q. Eulerian-Eulerian Model of 2D Normal Shock wave through a particle cloud. Master's thesis. San Diego State University, 2012.

[2] Shotorban B., Jacobs, G.B., Ortiz, O., Truong Q. An Eulerian model for particles nonsiotermally carried by a compressible fluid. International Journal of Heat and Mass Transfer, 65:845-854, 2013.

[3] Jacobs, G.B., Don, W.S. A High Order WENO-Z Finite Difference Based Particle-Source-in-Cell Method for Computation of Particle-Laden Flows with Shocks, J. Comp. Phys., 228 (5), 2009.

[4] Shu, C.W. High Order Weighted Essentially Nonoscillatory Scheme for Convection Dominated Problems. Society for industrial and Applied Mathematics. 51(1), 82-126, 2009.

[5] Ortiz, O. Eulerian-Eulerian Model of 1D Compressible Particle-Laden Flow: Running Shock Impingning on a Cloud of Particles. Master's thesis. San Diego State University, 2011.